



# Radiological imaging in multiple myeloma: review of the state-of-the-art

Francesca Di Giuliano<sup>1</sup> · Eliseo Picchi<sup>2,3</sup> · Massimo Muto<sup>4,5</sup> · Antonello Calcagni<sup>2,3</sup> · Valentina Ferrazzoli<sup>1</sup> · Valerio Da Ros<sup>3,6</sup> · Silvia Minosse<sup>3</sup> · Agostino Chiaravalloti<sup>3,7</sup> · Francesco Garaci<sup>1,8</sup> · Roberto Floris<sup>2,3</sup> · Mario Muto<sup>5</sup>

Received: 21 December 2019 / Accepted: 26 March 2020 / Published online: 21 April 2020

© Springer-Verlag GmbH Germany, part of Springer Nature 2020

## Abstract

**Purpose** Multiple myeloma is a type of blood cancer arising from the uncontrolled clonal proliferation of malignant plasma cells resulting in impaired hematopoiesis, hyper production of monoclonal protein, bone tissue destruction leading and renal system alterations up to kidney failure. The aim is to review the state-of-the-art of radiological imaging in multiple myeloma.

**Methods** Radiological techniques as well as the advancements in imaging technology have been reviewed and summarized. The main radiological findings of different imaging techniques in patients suffering from multiple myeloma are also illustrated.

**Results** Different radiological techniques provide structural and functional data. In the last years, conventional skeletal survey has gradually lost its utility and it has been replaced by whole body low-dose computed tomography which allows to identify also small lytic lesions, the medullary and the extramedullary involvement. Nowadays, magnetic resonance is the most sensitive imaging technique for detecting of skeletal as well as medullary involvement in patients with multiple myeloma. Thanks to the multiparametric evaluation (morphological, diffusion weighted and perfusion imaging sequences) and to the quantitative analysis, magnetic resonance imaging is proved to be useful in the early evaluation of response to therapy. Finally, positron emission tomography has greater sensibility compared to computed tomography as it provides quantitative data; however, the lower expression levels of the specific gene involved in the glycolysis pathway are associated with false-negative results with consequent underestimation of the disease.

**Conclusion** The only use of the advanced combined multimodal imaging allows a better evaluation, staging and early assessment of treatment response in patients with multiple myeloma.

**Keywords** Multiple myeloma · MRI · CT · PET · Interventional radiology

## Key points

- Multiple myeloma (MM) is the main disorder of the bone marrow in adults representing about 1% of all neoplastic disease. MM is the second most common hematologic malignancy after chronic lymphatic leukemia.
- Conventional skeletal survey lacks of sensitivity, with a false-negative rate ranging from 30 to 70%, leading to misdiagnosis or underestimation of the disease stadium.
- Thanks to its greater sensitivity and high-contrast the whole-body low-dose computed tomography (WB-LD-CT) allows the evaluation of bone, medullary and extramedullary involvement in MM reducing the effective radiation dose.
- The whole-body magnetic resonance imaging (WB-MRI) is the most sensitive imaging technique for detecting skeletal and extra-skeletal MM invasion. Moreover, the multiparametric information obtained by MRI may be useful for assessment of treatment response by qualitative and quantitative analyses of the perfusion and diffusion data.
- 2-deoxy-2-[fluorine-18]fluoro-D-glucose positron emission tomography has been proved to report a good sensitivity and specificity for assessment of medullary and extramedullary disease in patients with MM and for assessment of treatment response.
- Interventional radiology can be useful in multiple myeloma specially to treat complications by percutaneous vertebroplasty, balloon kyphoplasty and radiofrequency.

✉ Eliseo Picchi  
eliseo.picchi@hotmail.it

## Introduction

Multiple myeloma (MM) is a plasma cell dyscrasia (PCD) characterized by the uncontrolled clonal proliferation of abnormal plasma cells, impaired hematopoiesis with hyper production of monoclonal protein, bone tissue production and destruction leading to renal system impairment up to kidney failure. MM is the main bone marrow disorder in adults, representing about 1% of all neoplastic disease [1], and the second most common hematologic malignancy after chronic lymphatic leukemia; men are more likely to be affected than women and the pathology is more frequent in African Americans than Caucasians. Seventy percent of affected patients are over 60 years old [2]. The disease commonly evolves in subclinical form long before the symptomatic manifestation of multiorgan damage.

Osteolytic lesions are one of the most common signs of MM and the typical findings at radiological examinations. These lesions are mainly found in the axial skeleton and pelvis bones, less frequently in the arms and legs. In addition to causing severe bone pain, lytic lesions are responsible for pathological fractures, often involving vertebral soma and leading to complications such as spinal cord compression [1].

Over the past three decades, there have been relevant advances in radiological techniques and technology, above all in CT and MRI which have completely replaced the conventional skeletal survey (CSS), improving early radiological diagnosis of MM and in monitoring therapies.

The article is aimed at reviewing imaging techniques and radiological findings in MM focusing on more advanced imaging technologies.

## Classification and clinical history of plasma cell dyscrasias

Plasma cell dyscrasias (PCDs) are a heterogeneous group of monoclonal neoplasms originating from the most terminally differentiated B cells, whose primary function is to secrete antibodies to fight infections. Clonal cells form and secrete a single immunoglobulin (Ig) class or a polypeptide subunit of Ig that is usually detectable as a monoclonal protein (M protein) in serum or urine [3].

PCDs range from asymptomatic disorders, which can never manifest themselves clinically as monoclonal gammopathy of undetermined significance (MGUS), to intermediate forms, such as smoldering multiple myeloma (SMM), or more aggressive diseases with significant morbidity and mortality, such as plasma cell myeloma (Table 1). The classification of plasma cell neoplasms is based on a combination of clinical and pathological parameters that take into account the extent of the disease (clonal plasma cell burden and M-protein concentration) and evidence of end organ damage/dysfunction.

**Table 1** Classification of plasma cell dyscrasias according to the World Health Organization

1) Monoclonal gammopathy of undetermined significance (MGUS)
- IgM
- IgG/A
2) Waldenstrom macroglobulinemia
- Plasma cell myeloma
- Symptomatic myeloma
- Asymptomatic myeloma (smoldering)
- Nonsecretory myeloma
- Plasma cell leukemia
3) Plasmacytoma
- Solitary osseous plasmacytoma
- Extramedullary plasmacytoma
4) Immunoglobulin deposition disease
- Primary amyloidosis
- Systemic light and heavy chain deposition diseases
5) POEMS syndrome

Adapted from [Swerdlow et al. \(2016\) \[4\]](#)

Waldenstrom macroglobulinemia (WM) is an IgM monoclonal gammopathy; patients may suffer from a subclinical form of IgM MGUS but most patients become symptomatic during the disease course developing anemia, hyperviscosity and neuropathy [5].

Plasmacytoma is a tumor consisting of monoclonal plasma cells, developing secondary to MM or as a solitary form. The soft tissue lesions may arise in the bone, most commonly in the spine, or in extra-osseous locations, making diagnosis challenging. The prognosis and treatment of solitary bone plasmacytomas are very different from solitary extramedullary lesions even if both forms respond to treatment very well; however, the osseous form has a poorer prognosis due to its higher rate of evolution in MM [6].

PCD with light- or heavy-chain monoclonal Ig secretion may be associated with deposition diseases. Primary systemic amyloidosis is due to the interstitial deposition of light chain Ig as fibrillary amyloid in multiple organs, except for the central nervous system (CNS); 12–30% of MM patients have coexistent symptomatic or subclinical amyloidosis [7]. Heavy chains may also deposit in a variety of tissues, though heavy-chain deposition diseases are the least common MM-related diseases; clinical manifestations vary according to the heavy chain type. However, accumulation in the renal parenchyma is mainly responsible for clinical symptoms [8].

POEMS syndrome is paraneoplastic syndrome associated with plasma cell disorders such as MM, always characterized by polyneuropathy and very frequently by bone sclerotic lesions; organomegaly, endocrinopathy and skin alterations are minor criteria for diagnosis.

## Diagnosis and diagnostic criteria

PC disorders are classified according to the International Myeloma Working Group (IMWG) criteria (Table 2), which integrate blood and urine tests, bone marrow aspiration or biopsy and radiological imaging findings. Integrated diagnosis led to a more precise identification of the disease, which is essential for deciding when the treatment has to be started [9].

The diagnosis of MGUS and smoldering myeloma requires the absence of hypercalcemia, renal failure, anemia and bone lesions (CRAB features) and no signs of amyloidosis; they differ in monoclonal protein levels and bone marrow plasma cell percentage.

MM is defined by the percentage of bone marrow plasma cells  $\geq 10\%$  or biopsy-proven bony or extramedullary plasmacytoma; this is a necessary criterion; therefore, if bone marrow plasma cells are less than 10% and biopsy is not possible, follow-up is required. The second necessary criterion for diagnosis is the evidence of end organ damage, identified by CRAB criteria; in their absence, biomarkers of malignancy are alternatively considered and, among these, radiological markers are crucial. In fact, the presence of more than 1 focal lesion  $\geq 5$  mm in size on MRI is an alternative criterion, and it allows prompt diagnosis before symptom onset.

Related plasma cell proliferative disorders, such as AL amyloidosis and POEMS, may exhibit CRAB-like features even with low-levels of bone marrow plasmacytosis; in these cases, the IMWG criteria for MM diagnosis are not met.

In 2014, the criteria for the diagnosis of MM were updated; since then, more effective imaging techniques have been applied in the diagnostic algorithm, such as whole-body low-dose computed tomography (WBLD-CT), whole-body MRI (WB-MRI) and 18F-fluorodeoxyglucose positron emission tomography (18F-FDG-PET) [9, 10]. Therefore, the radiological criteria for the diagnosis of MM depend on the imaging technology chosen [11].

**Table 2** Diagnostic criteria for multiple myeloma

1) Clonal bone marrow plasma cell $\geq 10\%$ or
2) Biopsy-proven bony or extramedullary plasmacytoma and
(a) Any one or more of the following myeloma-related events:
- Hypercalcemia (C)
- Renal insufficiency (R)
- Anemia (A)
- Bone lesions (B)
(b) Any one or more of the following biomarkers of malignancy:
- More than 60% clonal bone marrow plasma cells (S)
- Involved/uninvolved serum-free light chain ratio $\geq 100$ (Li)
- More than 1 focal lesion on MRI (each focal lesion must be $\geq 5$ mm in size) (M)

## Conventional radiography

Since the first myeloma-related bone lesion observed on radiographs by Weber in 1903, CSS has been extensively used for diagnosis and follow-up in MM and considered the gold standard technique [12]. However, it lacks sensitivity, with a false-negative rate ranging from 30 to 70%, leading to misdiagnosis or underestimation of the disease stage [13]. As a matter of fact, myeloma-related bone lesions become noticeable on conventional radiography only when 30–50% of bone mineral density is lost [14].

Bone lesions in myeloma patients typically appear in flat bones (skull and pelvis) as punched-out ovoidal lytic areas without sclerosis of the surrounding bone (Fig. 1), while bone lesions in long bones have different appearances such as endosteal scalloping, small lytic lesions, mottled areas of small multiple lesions or large destructive lesions [15, 16]. In a CSS, almost 80% of myeloma patients have skeletal involvement that most commonly affects the following sites: 65% vertebrae, 45% ribs, 40% skull, 40% shoulders, 30% pelvis and 25% long bones, while radiographic detectable radiographic lesions are rare in the elbows and knees [1].

According to the IMWG guidelines, the CSS has to include a posteroanterior view of the chest, anteroposterior and lateral views of the spine, humeri, femora and skull and anteroposterior view of the pelvis [1].

CSS still has several limitations: the main concern is that it cannot be used for the assessment of response to therapy of the lytic bone lesions which rarely show healing [17]. Other limitations include non-optimal view of some bone structures, low reproducibility, long time on the Bucky table and poor tolerance by aching patients at the different radiograph positions [15]. A further limit is the low specificity in the assessment of complications such as vertebral fracture, where radiography is not able to distinguish whether the cause is the osteoporosis, the corticosteroids treatment or a site of myeloma [1, 18]. For these reasons, starting from 2017 that is after the publication of ESMO Clinical Practice Guidelines, the conventional radiography can be used in myeloma diagnosis and staging only if CT scan is not available [9].

## Computed tomography

The choice of imaging modalities in the diagnosis and follow-up of MM is related to the availability and affordability of the different techniques. Certainly, CT provides higher sensitivity and more useful information than conventional radiography when assessing lytic bone lesions related to MM (Fig. 2). In 1985, Schreiman et al. reviewed the radiological exams of 32 patients affected by MM undergoing CT and showed that standard-dose CT revealed more bone lesions than CSS [19]. However, the cumulative radiation dose from standard CT is substantial for MM patients, with an effective dose range of

**Fig. 1** Skull radiographs on lateral (a) and frontal (b) projection showing the typical “punched out” appearance of bone lesions in multiple myeloma with uncountable small, well-circumscribed lytic lesions without sclerosing of the surrounding bone



25.5 to 36.6 mSv [20]. To overcome these limits, in recent years, the WBLDCT for skeletal investigation replaced conventional radiography and standard whole-body CT; this is made possible by the high contrast between the bone marrow tissues and the surrounding bones. In 2005, Horger et al. performed the first multidetector WBLDCT, with standard tube voltage (120 kV) and different low tube current (40–70 mAs) obtaining an effective radiation dose ranged between 4.1 and 7.5 mSv: these values were closely related to the tube current [21]. In 2008, Kropil reduced the tube voltage to 100 kV with time current of 100 mAs and automatic dose modulation: the mean-effective radiation dose was approximately 4.8 mSv [22]. Certainly, the most accurate comparison between image quality and effect of CT parameters (kV and mAs) has been performed by Gleeson et al. who applied 14 different WBLDCT protocols on a single cadaver and obtained a mean dose of 4.5 mSv further reducible to 1.74 mSv using 140 kV/14mAs, automated modulation of the tube current and a moderately sharp reconstruction algorithm [23].

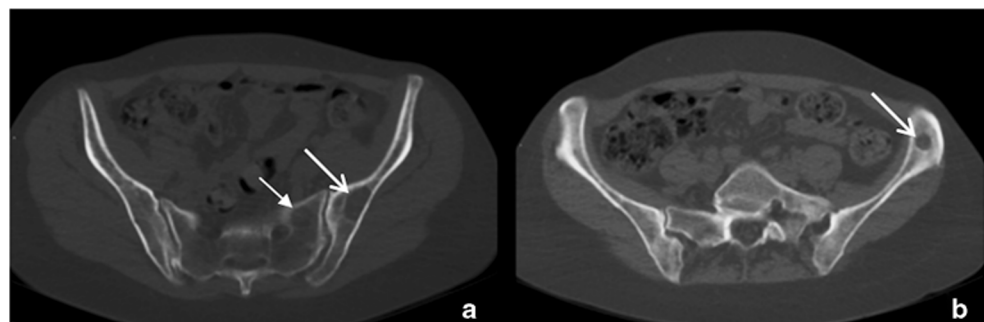
However, no validation setting for WBLDCT has been provided so far and today the effective radiation dose is related to clinical experience and the type of CT scanner.

The WBLDCT was included in the 2014 IMWG criteria for the MM definition [24]; WBLDCT is more sensitive than

radiographic CSS and it causes treatment modification in 18–61% of patients [25]; in a recent multicenter study, using whole body CT, Hillengass et al. reported that 20–25% of patients with negative skeletal survey had destructive bone lesions at CT [26].

In addition to the easy detection of osteolytic lesions, the WBLDCT allows the assessment of early bone marrow abnormalities in long bones which only become visible belatedly on conventional radiographies [20]. Myeloma lesions in the bone marrow are generally hyperdense (mean 55HU) in adults, contrasting healthy yellow marrow which typically appears hypodense (–30 HU to –100 HU) [27]. Nevertheless, according to HU of lytic lesions, Zambello et al. recognized two different patterns of lesions: the first with trabecular bone replaced by fat (HU lesion < 0) and the second with cell infiltration (HU > 0), of which the latter detected by <sup>18</sup>F-FDG uptake at PET and low apparent diffusion coefficient (ADC) at MRI [28]. Attention must be paid to the bone alterations previously identified as hypodense lytic bone lesions because they might become hyperdense, during the follow-up, showing infiltrative effects on the contiguous bones: therefore, there is a strong relationship between hypodense and hyperdense lesions in MM where the hypodense (or fat-rich) lesions seem to be an early stage that anticipates the

**Fig. 2** Axial CT scan images of pelvis showing a focal lytic lesion in right part of sacrum (white closed arrow in a) and two focal lytic lesions on left iliac wing (white open arrow in image a) and iliac crest (white open arrow in image b), respectively





hyperdense (or infiltrative) ones [28]. Despite these intriguing assumptions, the IMWG criteria do not define the specific density of myeloma lesions.

The IMWG criteria state that the definition of MM lesion is an osteolytic alteration with a diameter of at least 5 mm, without sclerosis of the surrounding bone [24]. Thanks to its high spatial and contrast resolution, WBLDCT allows to identify a single 5-mm lytic lesion unlike the CSS; however, even though this radiological condition is quite common, it is not strong enough to decide whether patients should undergo systemic therapy, thereby a short follow-up is essential [29, 30].

In addition to bone involvement, the WBLDCT allows the evaluation of any possible extramedullary involvement since MM may frequently appear as a para-osseous soft-tissue mass along bony structures such as ribs, spine, pelvic bones, in facial bones or along the extremity bones [31]. Radiologists must be aware of atypical manifestation of MM as localization in the lung, pleural lining, meninges as well as abdominal organ: in the last scenario, to avoid underestimating the disease, the administration of contrast medium is required.

WBLDCT should be performed with a multidetector CT scanner with at least 16 detector rows, with a field of view from the skull to the proximal tibial metaphysis; collimation should be set between 0.5 and 1.5 mm. During WBLDCT, Mouloupoulos et al. have suggested a voltage of 120 kV and a current between 50 and 75 mAs, even if they have recognized that other technical factors might achieve equal results [10]. Attention must be paid to the reconstructed images. While some authors use the middle-frequency kernel to analyze the thinner collimation data, having good radiological images at different window settings [21, 32], other investigators use two different kernels, the first with high spatial frequency convolution (for bone analysis) and the second with smoother convolution kernel (for soft tissue assessment). No contrast agents are needed for this examination.

As mentioned before, for a correct and precise evaluation of long bone involvement in MM, it is important to include the humeri and the tibia in the WBLDCT field of view; attention must be paid to the patient's positioning during the WBLDCT scan in order to rightly show the thoraco-lumbar spine and skull avoiding the weakening of the CT beam as well as the appearance of hardening and streaking artifacts: to achieve these results, the upper limbs must be placed in front of the body with folded hands.

Several clinical conditions (Table 3), which may temporarily or permanently affect bone density, must be excluded during the evaluation and interpretation of WBLDCT as reported in Table 3. Particular attention should be paid to fat deposits, small bone hemangiomas, Modic changes in the vertebral endplates and biopsy site that can mimic hypodense MM lesions [10].

Another interesting radiological technique for the study of MM lesions is the dual-energy CT (DECT) which is based on

**Table 3** Clinical conditions which affect the bone density

Temporary	Permanent
Chemotherapy	Malignancy (metastases, leukemia, lymphoma)
Granulocyte-CSF	Sickle cell disease
Erythropoietin	Paget disease
	Renal osteodystrophy
	Osteopetrosis
	Hyperthyroidism
	Hypoparathyroidism
	Poisoning (fluorosis)
	Osteopetrosis
	Mastocytosis

CSF colony-stimulating factor

the energy dependence of X-ray attenuation of two different photon spectra which allow the differentiation of substances with a high atomic number [33, 34]. Even though DECT was conceived in 1976, it was not much used in clinical settings due to its several technical limitations until the introduction of second-generation dual-source CT scanners with better spectral separation of radiological beams [35, 36]. These kinds of scanners use a tube current of 140 kV for the high-energy scan and of 100 kV for the low-energy scan, to reduce artifacts in anatomical sites with strong attenuation of radiological beams and to lead, on the other hand, to a larger overlap of radiological spectra; finally, a tin prefiltration is commonly used to reduce the radiation dose and increase the mean photon energy as well as spectral separation [37].

Nowadays, thanks to the introduction of the third-generation CT scanner, with usually paired current of 70 kV and 150 kV and a tin filter for the highest current, a better energy separation is achieved which allows greater dual-energy spectral contrast and thereby a more accurate decomposition of anatomical structures with different atomic number. Specifically, the application of the virtual non-calcium (VNCa) technique allows the evaluation of the bone marrow infiltration in MM and MGUS after the subtraction of the spongiotic bone. Subsequently, from the DECT, image dataset may be performed:

- quantitative analysis: based on the position of region of interest and assessment of Hounsfield units attenuation;
- qualitative analysis: using a color-coded map.

To our knowledge, there are only two studies on DECT and MM. The former was performed by Thomas et al. in 2015 who found a significant improvement in sensitivity for detection of bone marrow infiltration by MM compared to conventional CT [38]. The latter is a recent analysis of DECT performed on patients affected by MM or MGUS that has shown

excellent diagnostic performance for the evaluation of bone marrow lesions by visual and ROI-based analyses [37]. Kosmala et al. investigated possible correlations between bone marrow attenuation values emerged from DECT and MRI patterns in patients with multiple myeloma: from their analyses come out that, although the bone marrow VNCA attenuation values are different and depending on the imaging pattern, only diffuse bone marrow involvement can be determined using DECT [39].

Although nowadays this technique has interesting clinical applications, it is not used in the daily routine for several reasons, such as the limited availability of third-generation CT scanners and the presence of beam-hardening artifacts.

To overcome some limitations of DECT, a photon-counting detector CT using cadmium-base semiconductors has been developed: this new technology reduces the electronic noise and misregistration artifacts which frequently occur in DECT, reducing the effective radiation dose and increasing anatomical resolution and the contrast-to-noise ratio [40]. However, the increase in time for image reconstruction and interpretation is responsible for the limited use of this technology [41].

## Magnetic resonance imaging

The role of MRI has gained increasing interest and importance over the last years, and since 2014, the IMWG included MRI in the new diagnostic criteria. MRI is the most sensitive and specific imaging technique for the early detection of MM bone marrow infiltration, as it assesses bone marrow cellularity and composition [42, 43]. Several studies have shown a greater sensitivity of MRI than CSS, CT, and PET/CT in detecting MM lesions [13, 44, 45]. Recently, Rasche et al. reported that a lower expression of hexokinase 2, a gene involved in the glycolysis pathway, is associated with false-negative FDG-PET in MM with consequent underestimation of the disease [46]. Even if the prognostic significance of the lesion discrepancy in between MRI and FDG/CT has not yet been understood, WB-MRI determines the greatest increase in quality life years compared to CT or PET/CT [47].

Since 2016, the IMWG has confirmed the WB-MRI as the most sensitive imaging technique for detecting skeletal MM invasion: more than one focal lesion of at least of 5 mm detected by MRI is enough to define MM [24, 48]. On the other hand, the finding of equivocal or smaller (< 5 mm) lesions should be verified by MRI within 3–6 months [48, 49].

## The role of conventional MRI sequences

The standard MRI protocol for the evaluation of axial skeleton in MM includes Spin Echo T1- and T2-weighted images and the Short Tau Inversion Recovery (STIR) images; usually,

contrast-enhanced imaging is not performed as it does not increase bone lesion detection [44, 50]. There are three fat suppression techniques [51]:

1. Chemical shift-based fat suppression:
  - Chemical shift selective;
  - Water excitation;
  - Dixon;
2. Inversion-based fat suppression (STIR);
3. Hybrid techniques (spectral attenuated inversion recovery and spectral pre-saturation with inversion recovery).

Shah and Hanrahan reported more homogenous fat suppression (FS) for the STIR sequences with respect to the fat-saturated T2-weighted images [52]; moreover, although STIR images have lower spatial resolution than the FS sequences, they are not affected by the inhomogeneity of the magnetic field and allows to clearly assess and immediately recent fractures due to the appearance of intraspongious edema (Fig. 3).

The main limitation of MRI is the long examination period in patients often suffering from the underlying disease; to overcome this drawback, to obtain better-quality images and to correct many confounding factors, Dixon-type pulse sequences have been developed (Fig. 4) [53, 54].

Dixon-type sequences are characterized by a better signal-to-noise ratio (SNR) compared to chemical shift selective sequences [55]. Dixon sequences are based on the chemical shift of tissues and exploit the fact that water and fat molecules precess at different rates.

Thanks to the tissue's physical properties and mathematical analysis, it is possible to get four different weighted images by acquiring one:

1. In-phase (IP);
2. Opposed phase (OP);
3. Water-only images (WO);
4. Fat-only images (FO);

Dixon techniques could be

1. one echo (single-point Dixon)
2. two echoes (two-point Dixon)
3. more echoes (multi-point Dixon)

These features offer Dixon sequences the possibility of quantifying the amount of fat and obtaining WO and FO thanks to post-processing [56, 57]. Bray et al. used Dixon-pulse sequences to evaluate focal MM lesions and found good diagnostic accuracy on fat-only images for the detection of MM lesions [58]. Huijgen et al. and Lee et al. compared, respectively, the T1 and T2-w and only T2-w fat saturation

**Fig. 3** Sagittal T1-weighted (a) and sagittal T2-STIR (b) images show T2 hyperintensity of the superior endplate fracture of T6 in a 57-year-old man with previous diagnosis of MM. To note the convex bowing profile of the posterior wall of T6 vertebra



techniques with the Dixon technique and concluded that Dixon was superior in fat-suppression quality and in identifying focal skeletal lesions [59, 60].

T2-weighted FO Dixon images have shown a significantly higher contrast than T1-weighted images and result to be more efficient at detecting focal MM lesions [61]. The comparison

between T2w Dixon FO to T1w images has shown a higher contrast-to-noise ratio for Dixon's images and not significantly lower diagnostic performance [62]. These evidences suggest that for the assessment of MM focal lesions, the T2w Dixon FO images result to be effective and, if non-inferiority with respect to other fat-suppressed sequences will

**Fig. 4** T1 Dixon images in 51-year-old man with diffuse MM and lytic bone changes. a Dixon T1-weighted; b Dixon T1-weighted fat-only; c Dixon T1-weighted water-only; d Dixon T1-weighted out-of-phase. The images show multiple spinal lesions showing low signal intensity in the four different T1-weighted images due to the high cellularity of MM spinal lesions and reduced amount of fat





be proved and they could become a valid alternative to the actual standard protocol.

In MY-RADS, Messiou et al. have suggested acquiring sagittal T1w, T2w, T2w fat-suppressed sequences of whole spine and T1 gradient-echo Dixon and DWI from vertex to knee, with a protocol that lasts about 30 min and allows a complete skull evaluation. However, in case of suspicion of extramedullary disease, it is possible to acquire additional sequences [63].

All the above-mentioned assumptions suggest continuing to study the comparisons between standard sequences to Dixon's images to improve our knowledge and to determine if it is possible to use only the latter to significantly reduce acquisition times.

Active MM lesions in the marrow usually appear hypointense on T1-weighted images, hyperintense on T2-weighted and sequences with fat saturation compared to healthy marrow, due to the high cellularity, high amount of water and reduced amount of fat [64, 65].

Analyzing the conventional MR images, five different patterns (Fig. 5) were identified which related to both the type of bone marrow involvement by MM and the histological findings [66–68]. The five patterns are

- a) the normal appearing marrow;
- b) the focal pattern;
- c) the diffuse pattern;
- d) the salt-and-pepper or micronodular pattern;
- e) the combination of focal lesions in a diffuse pattern.

Several authors have found correlation between the MRI pattern and the number of lesions with the stage of disease and survival, confirming the prognostic value of MRI [44, 68, 69]: in particular, the diffuse pattern at MRI correlates with more advanced disease and worse prognosis.

However, the bone marrow infiltration in MM is mostly inhomogeneous and the ability to identify areas of high versus low local plasma cell infiltration is essential: the multiparametric MR imaging, composed by diffusion

weighted imaging (DWI) and dynamic contrast-enhanced (DCE) imaging, may offer information on bone marrow cellularity and perfusion thus increasing the lesion detection rate [70].

### The role of DWI

DWI is a functional MR technique, based on the Brownian motion, which allows to evaluate the molecular architecture of human tissues. By assessing the water diffusion in the interstitium, the DWI is able to quantify the tissues' cellularity. Typically, solid tumors are characterized by small interstitium and therefore by a restricted water diffusivity [71]. Takahara et al., using a short time inversion recovery-echo planar imaging sequence with body signal suppression (DWIBS), introduced whole-body DW-MRI as a method for cancer screening [72]. Although DWIBS is a fast and sensitive technique with high anatomical coverage, it remains of limited use in diagnosis; nevertheless, DWIBS could play a key role in the evaluation of response to therapy and in monitoring disease [73–75].

In patients with MM, the optimal b-value, to maximize the contrast between normal and infiltrated marrow, is about  $1400 \text{ s/mm}^2$ ; however, since high b-value determines a significant lengthening of the scan times and the reduction of the signal-to-noise ratio, Messiou and Kaiser have proposed a b-value of  $900 \text{ s/mm}^2$  [74, 76].

DWI analysis is qualitative and quantitative. The qualitative DWI analysis is usually performed by visual assessment of the signal intensity on the highest available b-value image: high signal intensity on DWI means restriction of the water diffusivity and thereby high cellularity [65, 77]. During the qualitative evaluation of DWI, radiologists must pay attention to the “T2-shine through” effect related to the amount of free water as well as to the intrinsic T2 relaxation time of the tissue; to avoid misinterpretation, the qualitative analysis has to be correlated to the apparent diffusion coefficient (ADC) map and conventional morphological sequences. Care should be taken when evaluating hyperintense DWI lesions in MM patients since fractures, infection, osteoarthritis, vertebral

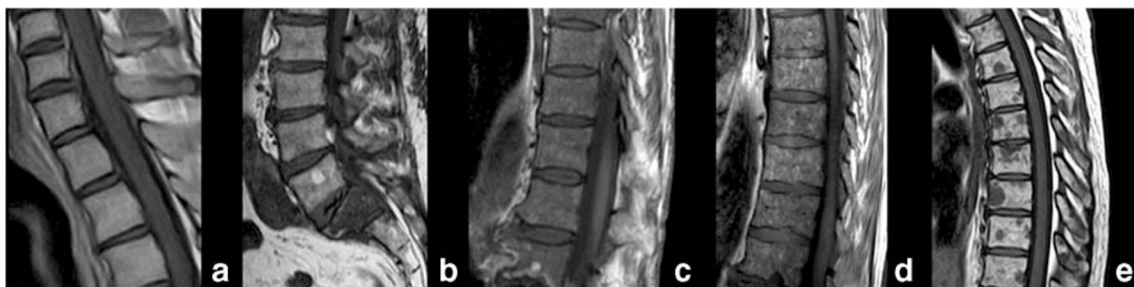


**Fig. 5** Multiple myeloma MRI pattern. **a** Sagittal T1-weighted image, normal spine pattern; **b** sagittal T1-weighted image shows focal MM pattern at the level of S1; **c** sagittal T1-weighted image shows diffuse

spinal pattern; **d** sagittal T1-weighted image shows the “salt-and-pepper” pattern; **e** sagittal T1-weighted image shows MM mixed pattern



hemangiomas, cysts, peri-focal metal artifacts and focal areas of fat-poor bone marrow cause false-positive results [78, 79].

The quantitative analysis is based on the evaluation of the (ADC) map which represents, for each pixel, the diffusion of the water molecules: being the interstitium reduced in hypercellular neoplasms, the ADC values will be low (Fig. 6). However, the ADC maps are affected by several variables such as tissue architecture, cell size, cytoplasm viscosity and bulk flow in capillaries [74].

Typically, MM bone lesions are characterized by hyperintensity on DWI sequences and high ADC value due to reduction of adipocytes, destruction of trabecular bone and high cellularity [80]. Early response to treatment is characterized by a further increase in ADC values (due to plasma cell death and increased interstitium) and hyperintensity on DWI (due to the “T2-shine through” therapy-related effect). The later response, several weeks after therapy, is characterized by the normalization of the bone marrow appearance [81].

Despite the IMWG recommends using T1, T2, STIR and T1 sequences after the administration of the gadolinium-based contrast agent for evaluation of soft tissue involvement, the last consensus statement suggests using the DWI sequences, also considering the results of Pearce et Dutoit who detected more lesions by DWI analysis than conventional STIR and contrast-enhanced MRI [65, 82]. The European myeloma network guidelines recommend the use of DWI in asymptomatic patients suffering from smoldering MM without lytic lesions detectable at WB-CT [83]: the detection on DWI of more than one focal bone lesion, with a diameter of at least 5 mm, allows diagnosis of bone marrow involvement in myelomatous

patients while equivocal bone lesions should be imaged again in 3 to 6 months [49].

Even though whole-body DW-MRI shows great sensitivity for bone involvement detection, even in asymptomatic patients, the debate remains still open on its specificity due the conflicting data reported in the literature [82, 84, 85].

Surely, the DW-WB-MRI, in addition to conventional MR sequences, improves the diagnostic accuracy after treatment in the assessment of early response and in the disease monitoring by evaluating the signal intensity of the pathological tissue on the DWI and ADC map.

### The role of dynamic contrast-enhanced MRI

Contrast-enhanced MRI is not routinely performed in myelomatous patients because it does not increase the rate of lesion detection (Fig. 7) [50]; however, the use of contrast medium is essential when the lesions have a compressive effect on the spinal cord or involve paravertebral soft tissues.

In patients suffering from MM with renal function impairment, the administration of gadolinium-based contrast agent is not forbidden if the radiologist follows the current guidelines [86]: renal function is not affected by contrast medium in patients with asymptomatic MM and also the use of the linear paramagnetic contrast agent has no negative prognostic effects on patients with plasma cell dyscrasias.

However, since MM is a solid tumor, it has an alteration of the physiological perfusion pattern due to aberrant angiogenesis and pathological vessel permeability. Dynamic contrast-enhanced (DCE) MRI allows evaluating tumoral

**Fig. 6** Qualitatively DWIBS (a, c) and ADC (b, d) images in 45-year-old woman showing multiple areas of high signal intensity on DWI and reduction of ADC values corresponding to areas of high cellularity

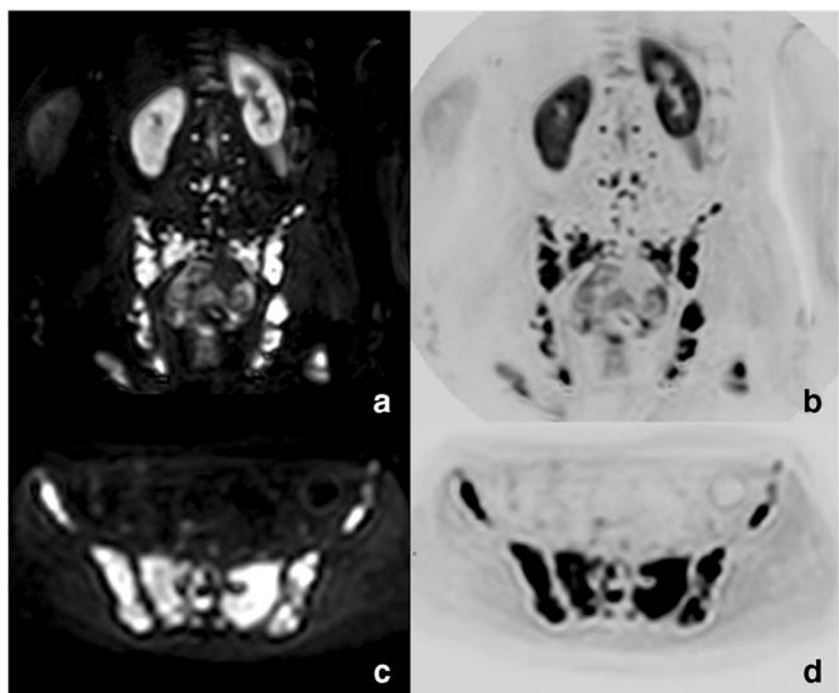
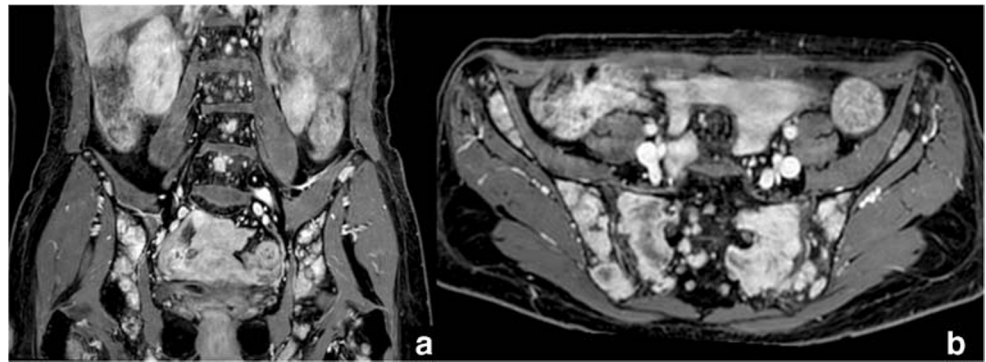


**Fig. 7** Coronal (a) and axial (b) T1-fat suppressed images with after administration of GBCA in MM patient show diffuse areas of contrast enhancement of the pelvic bones



neoangiogenesis by providing useful information on tissues and perfusion characteristics [87]. The passage of gadolinium-based contrast agent determines temporal variations of the time-intensity curve (TIC) which are related to the structures of the analyzed tissue.

By evaluating the shape of TIC, based on the tissue wash-in, wash-out and plateau, the qualitative analysis of the tissue is performed: MM bone lesions are usually characterized by steep and rapid wash-in with quick wash-out (type 4); less frequently type 3 (steep and rapid wash-in and wash-out plateau) or 5 (quick but less intense wash-in and late stable or increasing enhancement) are shown [80, 88, 89]. Moreover, the quantitative analysis of DCE-MRI can be performed using the pharmacokinetic mathematical model as suggested by Garcia-Figueiras [90].

This functional MRI technique, together with the DWIBS, may be useful in the early evaluation of the response to treatment by qualitative and quantitative analyses of the perfusion data.

Nowadays, MRI, thanks to the multiparametric analysis, is recommended as first-line imaging for the evaluation of patients with suspected asymptomatic myeloma or solitary bone plasmacytoma, and in the United Kingdom, whole-body MRI is considered the first imaging modality for patient with suspected diagnosis of MM [1, 47, 91].

The increasing role of WB-MRI in patients suffering from MM is also suggested by the recent discussion on the Myeloma Response Assessment and Diagnosis System (MY-RADS) with the aim to promote standardization in the acquisition, interpretation and reporting of WB-MRI [63].

## PET-CT

2-Deoxy-2-[18F] fluoro-D-glucose ([18F] FDG) is a positron emitting radiopharmaceutical containing no-carrier added radioactive 2-deoxy-2-[18F] fluoro-D-glucose. It is administered by intravenous injection and is concentrated in cells that rely upon glucose as an energy source, or in cells whose

glucose dependence increases under pathophysiological conditions, such as tumors [92].

Since its introduction into the clinical routine in the early 1990s, [18F]FDG-PET/CT has proven to be a useful diagnostic tool for staging and restaging several hematological malignancies, such as Hodgkin's disease (HD) and diffuse large B cell lymphoma (DLBCL) [93]. On the other hand, in other types of solid tumors with mild or low [18F] FDG avidity, the use of [18F] FDG PET showed limited diagnostic accuracy [94]. In a paper aimed to evaluate the [18F] FDG avidity in different types of lymphomas, the avidity decreased from 100% in HD and DLBCL to 50% in marginal zone lymphoma [94]. As for MM, the role of [18F] FDG has not been clearly established due to the variety of metabolic patterns observed in this disease. Treatment of MM cell cultures with glycolysis inhibitor and oxidative phosphorylation, such as 2-deoxyglucose (2DG), increased MM cell apoptosis in a dose-dependent manner, thus suggesting that ATP production and viability are reduced in MM cells after adding 2DG [95–97]. Another effect of 2DG is that its phosphorylated form cannot be metabolized and subsequently accumulates in the cell and interferes with the glycolytic pathway [96, 97]. These findings suggest that glucose metabolism is significantly increased in MM. On the other hand, human MM cells in vitro show an excess of NH<sub>4</sub><sup>+</sup> produced from glutamine, which leads to suppose that the metabolism of MM cells is also dependent on glutamine [98].

[18F] FDG demonstrated a good sensitivity and specificity for the detection of medullary and extramedullary disease in patients with MM as compared to X-rays, with PET imaging being superior in detecting bone lesions in 46% of patients (Fig. 8) [42]. In the same study, PET-CT enabled the detection of myelomatous lesions in areas out of the field of view of MRI in 35% of patients. By combining spine-pelvis MRI and 18F-FDG PET-CT, the ability to detect active MM sites, both medullary and extramedullary, was up to 92% high [42]. In another study of Moreau et al. performed on 134 patients, 18F-FDG PET/CT showed a lower detection rate being positive in 91% of cases vs. 95% of MRI [99]. On the other hand, an interesting finding of this research was the prognostic value

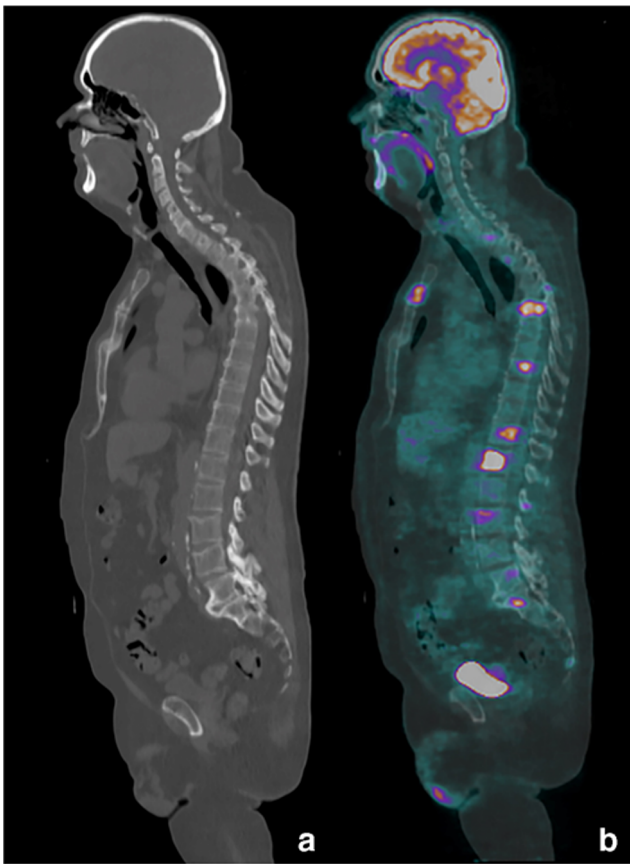


**Fig. 8** Sagittal slices of positron emission tomography/computer tomography (PET/CT) performed at staging showing in **a** no significant abnormalities of the bones in a patient affected by multiple myeloma (MM) in CT images. In **b**, fused PET/CT images show multiple areas of focal uptake of 2-deoxy-2-[18F] fluorogluucose (18F FDG) due to diffuse disease then confirmed at biopsy

of PET/CT after chemotherapy. Normalization of the 18F-FDG distribution during the treatment course and after three cycles was significantly related to progression free survival and overall survival [99]. A positive result at PET/CT was found to be a prognostic factor in a recent study in which at least three focal lesions at the diagnosis,  $SUV > 4.2$  and persistence of PET/CT positivity after auto-transplant were poor prognosticators [100, 101]. It is interesting to note that, before maintenance therapy, MRI became normal in 11% of patients with positive results at baseline while PET-CT normalization was described in 62% of the patients positive at baseline [99]. This finding could be explained considering that normalization of MRI findings in responding patients may take several months, and the sensitivity of MRI for the detection of remission may be reduced due to false-positive results [102]. False-positive findings can also occur in 18F-FDG PET/CT. Increased 18F-FDG uptake can be related to the artifacts (more frequently when there are bone metallic implants), infections, post-surgical or biopsy area, bone remodeling, fractures and, more frequently, the recent use of chemotherapy,

radiotherapy or growth factors that induce a false diffuse bone marrow pattern [103].

Several studies have investigated the potential role of other radiolabeled compounds. Luckerath et al. found that early reduction of 11C-methionine uptake but not 18F-FDG correlated with improved survival and reduced tumor burden in mice, suggesting that 11C-methionine is superior to 18F-FDG in very early assessment of response to anti-myeloma therapy [104]. (11)C-acetate showed a significant incremental value over (18)F-FDG (84.6% vs. 57.7%) for identifying patients with diffuse and focal symptomatic MM and was negative in patients with indolent smoldering MM and monoclonal gammopathy of unknown significance, suggesting possible advantages over 18F-FDG in the staging of patients with newly diagnosed MM [105]. 11C-Choline was tested in a limited pool of patients with MM with promising results. This radiolabeled compound allows specific evaluation of cell membrane proliferation and appears to be more sensitive than 18F-FDG, especially in detecting skull lesions [99].

## Interventional radiology in multiple myeloma

Patients affected by MM can frequently develop complications such as renal failure, hematologic alterations and bone lesions (osteolytic in up to 90% of myeloma patients) [83, 106, 107].

Unfortunately, bone lesions are characteristic of many pathologies, primary of the bone as well as secondary to other diseases. In order to have a diagnosis of the etiology, it is necessary to perform a biopsy which allows to discriminate between myeloma, solitary plasmacytoma or any other focal bone disease. Biopsy can be performed on focal lesions, removing bone, a small amount of fluid and cells, or at random location (bone marrow aspiration alone). [108]. When a focal lesion is not demonstrable, bone marrow aspiration is performed from the iliac crest, in order to evaluate and determine the representation of plasma cells [108, 109].

Biopsy is also necessary for the diagnosis of solitary extramedullary plasmacytoma (SEP), a rare soft tissue localization of plasmacytoma usually located in the head and neck, due to non-specific findings in MRI or CT [6, 110]. One of the main advantages of biopsy is that it is suitable for cytogenetic tests in order to detect numerical and structural chromosomal abnormalities/aberrations in bone marrow cells. The therapeutic approach and prognostic assessment have improved thanks to the cytogenetic analysis [111, 112].

Up to 90% of myeloma patients can develop osteolytic lesions and 70% of patients are affected by osteolytic-osteopenic disease of the spine, with high risk of fractures. It is thus especially important to treat the osteolytic bone disease and vertebral compression fractures (VCFs) in a timely



manner. Treatment of the spine is directed towards keeping the patient pain free, ambulatory and continent.

The main pathologic fracture sites are found in the thoracic and lumbar vertebrae (52%) and may develop spinal cord compression, with severe back pain and disability [113–115]. Spinal cord compression affects approximately 11–24% of MM patients with vertebral fractures and can determine neurological impairment: it is necessary to undergo MRI scan for spinal cord evaluation and CT scan for bone assessment [116–118]. Imaging should outline whether or not the spinal cord is involved, because if neurological structures are compromised, urgent surgical treatment is needed [6, 119].

The “International Society of Interventional Radiology, Committee on Standards of Practice” has established guidelines for the use of vertebral augmentation techniques as percutaneous vertebroplasty and balloon kyphoplasty in vertebral fractures [120]. These are image-guided percutaneous interventions that aim to achieve vertebral body stabilization by bone cement injection (polymethylmethacrylate, PMMA) directly (the so-called vertebroplasty) or after the inflation of a balloon in the vertebrae, to attempt to reduce the fracture before injecting the bone cement (kyphoplasty). These techniques have shown a high success rate with a positive outcome in 70–90% of cases and are focused on inducing pain relief and/or improving mobility and quality of life (Fig. 9) [120–122].

Another therapeutic option is radiofrequency ablation (RFA): by percutaneous access, a high frequency alternating current is transmitted to the pathologic vertebrae or bone to determine necrosis and obtain pain relief. Due to the possibility that RFA alone may cause instability, it has been proposed to combine RFA with vertebroplasty; good results has also been shown using RFA combined with kyphoplasty (Fig. 10) [123–125].

In accordance with “the American College of Radiology”, the major indication for vertebral augmentation is the treatment of symptomatic fractures refractory to medical therapy or secondly weakened and microfractured vertebral bodies. These techniques are not indicated when the patient shows

an infectious state (general or local) or presents an uncorrectable coagulopathy or allergy to bone cement. Complications are rare and occur in less than 10% of patients who could develop transient or, rarely, permanent neurological deficits, adjacent vertebral fractures and leakage of bone cement with secondary pulmonary embolism [126].

In conclusion, interventional radiology can be useful in the diagnosis and treatment of multiple myeloma helping to relieve pain and improving patient quality of life.

### Radiology in sanctuary site evaluation

CNS and testes are “sanctuary sites” for hematologic malignancies, as it is difficult to obtain sufficient concentrations of chemotherapy because of the presence of brain-blood and testicular-blood barrier, respectively.

CNS involvement is very rare (less than 1% of MM patients) and develops when the disease relapses or progresses in the majority of cases, not necessarily in advanced stages. CNS may be primarily or secondarily involved by a contiguous bone lesion in the cranial vault, skull base, nose or paranasal sinuses [127].

Primary CNS involvement may mimic dural masses, leptomenigeal disease and rarely intra-axial lesions, with non-specific findings; dural masses generally appear hyperdense on CT, iso- to hyperintense on T1-weighted images and iso- to hypointense on T2-weighted images, related to muscles and gray matter, with mild-marked enhancement. DWI is altered in lesions with high cellularity or with low nucleocytoplasmic ratio.

Dural involvement without adjacent bony lesions is rare and probably due to dissection along the meningeal layers; leptomenigeal spread is more likely hematogenous [128]. Cavernous sinus involvement is rare but it has been reported both in relapsing disease and at diagnosis, as a secondary extension of bone lesions or as a dural mass without bone involvement [129]. The onset of neurological symptoms requires contrast-enhanced MRI evaluation; however, considering the non-specific radiological manifestations and the false negative rate around 10%, MRI should be interpreted together

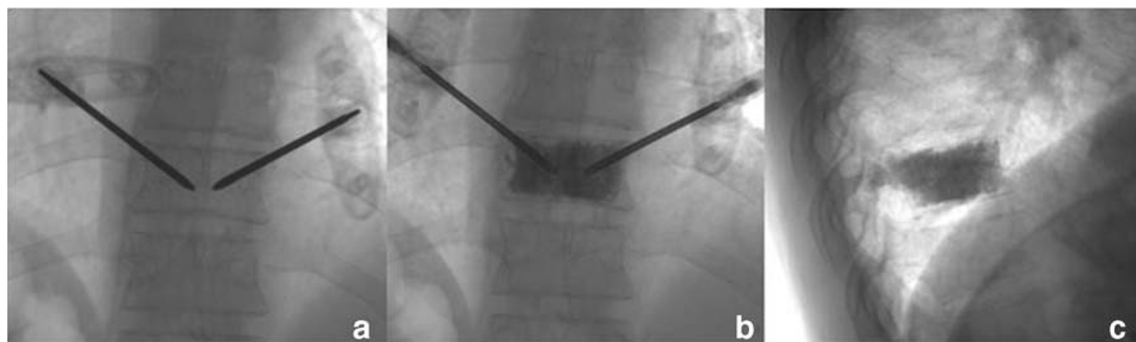


**Fig. 9** Antero-posterior (a, b) and lateral (c) fluoroscopic view of percutaneous vertebroplasty of D11. Bilateral transpedicular approach (a), bone cement injection (b). Lateral view of the end of procedure (c)



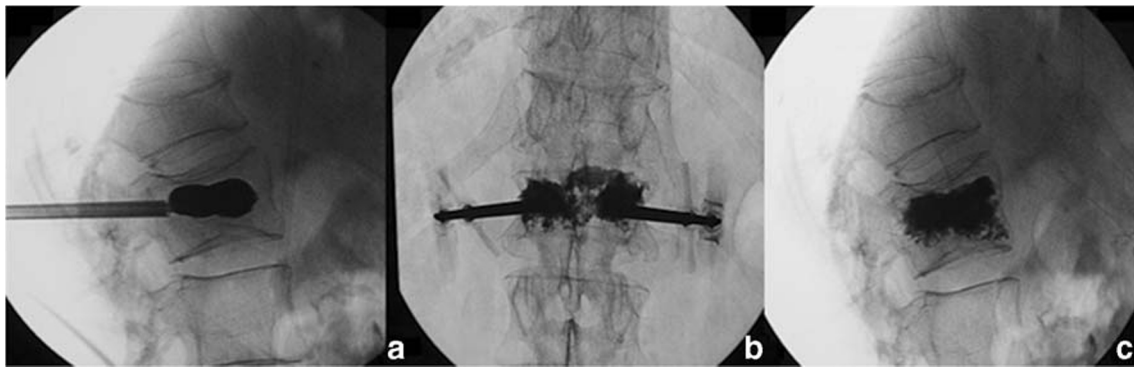


**Fig. 10** Lateral (a, c) and antero-posterior (b) fluoroscopic view of balloon kyphoplasty of L1. Positioning of vertebral balloon (a), bone cement injection (b). Lateral view of the end of procedure (c)

with the clinical history, pathological and CSF examination [130]. It is important to consider that pathological assessment is not always possible and CSF may be negative for plasma cells in CNS involvement. Moreover, neurological symptoms in MM patients may also be caused by metabolic alterations, amyloid deposits, hyperviscosity syndrome, myelin damage due to antibodies, drug toxicity [128]. For these reasons, radiological evaluation really takes part in an integrated diagnosis. CT is better than MRI in evaluating bone destruction, especially for subtle lesions, but MRI ensures the best assessment of bone marrow and intracranial disease.

A sanctuary site for hematologic malignancies is testis, because of their blood barrier. Testes are rarely involved in MM; however, a local mass appearance should raise suspicion and ultrasound should be performed [131, 132].

The timely identification of sanctuary site involvement, given its poor prognosis, is crucial to start a systemic treatment with new drugs. Immunomodulatory drugs and proteasome inhibitors seem to improve the outcome in CNS disease, more significantly in secondary involvement [133].

### Radiology in primary plasmacytoma

Plasmacytoma is a plasma cell dyscrasia that can be primary or secondary to disseminate MM. The secondary form is associated with a bone marrow PCs count  $\geq 10\%$ . In the primary form, there are no bone marrow plasmacytosis and CRAB features, and the localization may be osseous or non-osseous (extramedullary), with solitary or multiple lesions. Whole body evaluation is necessary in order to reveal multiple plasmacytomas that need systemic therapy.

The primary extramedullary form is very rare, and in the majority of cases, it develops in the upper aerodigestive tract (80%), rarely followed by the skin and gastrointestinal tract. The lesions present as soft tissue tumors with mass effect and infiltrative growth pattern in respect of the adjacent bone and adjacent tissues in larger lesions. Differential diagnosis with other malignant, primary or metastatic, lesions is challenging, especially in the upper aerodigestive tract, as the tissue is

commonly T2 hyperintense and mildly/markedly enhancing, with no specific features [134].

In staging the primary plasmacytoma that identifies regional lymphadenopathies, it is important for treatment planning in order to reduce recurrence.

The role of imaging is disease staging and monitoring, therefore to plan a patient-tailored treatment and identify early recurrence or progression.

### Radiology in MM-associated amyloidosis and POEMS syndrome

Light-chain amyloidosis (AL) is the most common systemic form and it is due to the production of Ig light chains (or their fragments) by clonal plasma cells. A total of 12–15% of MM patients develop symptomatic amyloidosis, but up to 30% of them suffer from an unrecognized subclinical form [7].

The organs that are most frequently affected in AL amyloidosis are the kidneys and the heart; however, virtually any tissue other than the brain can be involved and physical examination and tissue samples are crucial for the diagnosis [135].

Cardiac involvement in systemic amyloidosis has both therapeutic and prognostic significance. Heart involvement, clinically suspected, may be evaluated by cardiac MRI as it has quite specific kinetic of gadolinium enhancement in the myocardium; late gadolinium enhancement has been shown to precede the morphological alteration on the left ventricular thickness from amyloid deposition. Moreover, some features, as late gadolinium enhancement and myocardial edema, have been suggested as outcome predictors [136].

The kidneys are involved in 70% of patients with AL amyloidosis, which manifests itself as nephrotic syndrome and progressive renal failure. In renal amyloidosis, the kidneys are commonly atrophic with thinned cortex; renal enlargement may be seen, in the acute stage of the disease. Amorphous renal calcifications and focal parenchymal masses are rare. Renal vein thrombosis is a known complication and leads to renal failure [137, 138].

Pulmonary amyloidosis is more often a localized process that presents itself as a nodular pattern or alveolar septal form; the imaging features are non-specific and biopsy is often required for a conclusive diagnosis even in suggestive clinical settings. The nodular pattern has a benign natural history; alveolar septal amyloidosis leads more frequently to respiratory failure and has a more relevant prognostic significance [139].

POEMS syndrome is a paraneoplastic syndrome associated with plasma cell disorders such as MM. Polyneuropathy is a necessary major clinical feature needed together with the diagnosis of plasma cell disorder; a third major criterion is necessary for the diagnosis. The presence of sclerotic bone lesions is one of the major radiological features (95% of patients) and they appear densely sclerotic or lytic with a sclerotic rim; CT with bone window is more useful than PET-CT, since only lytic lesions have high metabolic activity. The presence of more than two lesions indicates the need for systemic therapy rather than radiotherapy to the single affected site, even if there is no bone marrow infiltration. For a conclusive diagnosis, at least one of the minor criteria is needed, among which are: organomegaly, endocrinopathies and skin alterations. CT imaging helps identify hepatosplenomegaly, adenopathy, effusions and ascites [140].

### Radiology in evaluating minimal residual disease

Thanks to improved therapies for MM, which have greatly enhanced the rates and depth of response, identification of minimal residual disease (MRD) has become important for guiding therapeutic decisions. Indeed, the presence of cells that survive after therapy may increase the risk of developing drug resistance and represents an adverse prognostic factor [141]. For these reasons, patients with MRD benefit from consolidation therapies and may take advantages of maintenance. MRD has been defined by the IMWG as the persistence or re-emergence of very low levels of cancer cells, equal to or about 1 tumor cell in at least  $10^5$  normal cells [142].

Bone marrow MRD is detected by two techniques based on flow cytometry and molecular technology; however, response evaluation based on single BM aspirates is not sufficient, as it is affected by the presence of patchy bone marrow infiltration or the possibility of extramedullary disease. For these reasons, imaging techniques can play a valuable role in defining MRD presence, both at the intramedullary and extramedullary levels, in addition to BM techniques.

MRI is sensitive in identifying diffuse BM infiltration or focal lesions at diagnosis; however, after treatment, it may be affected by necrosis and inflammatory reaction, with the same appearance of lesions in responding and not responding patients; for these reasons, MRI should be performed at least 3 months after therapy in order not to misinterpret the response [143].

Whole body MRI with DWI could be informative on the residual cell activity in BM and in extramedullary sites; however, the technique is not standardized, and compared with  $^{18}\text{F}$ -FDG PET-CT, the latter has demonstrated higher overall accuracy for determining remission status.

Considering the prediction of progression-free survival and overall survival,  $^{18}\text{F}$ -FDG PET-CT has been much better than MRI after treatment; PET/CT is applicable to all patients and is a sensitive study for detecting both bone lesions and extramedullary disease [99].

**Funding information** This research did not receive any specific grant from funding agencies in the public, commercial, or not-for-profit sectors.

### Compliance with ethical standards

**Conflict of interest** The authors declare that they have no conflict of interest.

**Ethical approval** For this type of study, formal consent is not required.

**Informed consent** Informed consent was obtained from all individual participants included in the study.

### References

1. Dimopoulos M, Terpos E, Comenzo RL et al (2009) International myeloma working group consensus statement and guidelines regarding the current role of imaging techniques in the diagnosis and monitoring of multiple myeloma. *Leukemia*
2. Palumbo A, Bringhen S, Ludwig H et al (2011) Personalized therapy in multiple myeloma according to patient age and vulnerability: a report of the European Myeloma Network (EMN). *Blood*
3. Lersbach RB (2010) Update on the diagnosis and classification of the plasma cell neoplasms. *Surg Pathol Clin*
4. Swerdlow SH, Campo E, Pileri SA et al (2016) The 2016 revision of the World Health Organization classification of lymphoid neoplasms. *Blood*
5. Castillo JJ, Treon SP (2019) What is new in the treatment of Waldenstrom macroglobulinemia? *Leukemia*. 33:2555–2562. <https://doi.org/10.1038/s41375-019-0592-8>
6. Grammatico S, Scalzulli E, Petrucci MT (2017) Mediterranean journal of hematology and infectious diseases solitary plasmacytoma. *Mediterr J Hematol Infect Dis*. <https://doi.org/10.4084/MJHID.2017.052>
7. Bahlis NJ, Lazarus HM (2006) Multiple myeloma-associated AL amyloidosis: is a distinctive therapeutic approach warranted? *Bone Marrow Transplant*
8. Rane S, Rana S, Mudrabettu C et al (2012) Heavy-chain deposition disease: a morphological, immunofluorescence and ultrastructural assessment. *Clin Kidney J*
9. Moreau P, San Miguel J, Sonneveld P et al (2017) Multiple myeloma: ESMO clinical practice guidelines for diagnosis, treatment and follow-up†. *Ann Oncol*. <https://doi.org/10.1093/annonc/mdx096>
10. Mouloupos LA, Koutoulidis V, Hillengass J, Zamagni E, Aquerreta JD, Roche CL, Lentzsch S, Moreau P, Cavo M, Miguel JS, Dimopoulos MA, Rajkumar SV, Durie BGM, Terpos E, Delorme S (2018) Recommendations for acquisition,

- interpretation and reporting of whole body low dose CT in patients with multiple myeloma and other plasma cell disorders: a report of the IMWG Bone Working Group. *Blood Cancer J* 8:1–9. <https://doi.org/10.1038/s41408-018-0124-1>
11. Chantry A, Kazmi M, Barrington S et al (2017) Guidelines for the use of imaging in the management of patients with myeloma. *Br J Haematol*. <https://doi.org/10.1111/bjh.14827>
  12. Weber FP (2005) Multiple myeloma (myelomatosis) with Bence-Jones proteid in the urine (myelopathic albumosuria of Bradshaw, Kahler's disease.). *J Pathol Bacteriol*. <https://doi.org/10.1002/path.1700090205>
  13. Baur-Melnyk A, Buhmann S, Becker C et al (2008) Whole-body MRI versus whole-body MDCT for staging of multiple myeloma. *Am J Roentgenol*. <https://doi.org/10.2214/AJR.07.2635>
  14. Baur-Melnyk A, Reiser M (2004) Staging of multiple myeloma with MRI: comparison to MSCT and conventional radiography . Staging des Mult myeloms mit der MRT Vergleich zur MSCT und zur konventionellen röntgendiagnostik
  15. Terpos E, Mouloupoulos LA, Dimopoulos MA (2011) Advances in imaging and the management of myeloma bone disease. *J Clin Oncol*
  16. Ågren B, Loqvist B, Bjorkstrand B et al (2009) Radiography and bone scintigraphy in bone marrow transplant multiple myeloma patients. *Acta Radiol*. <https://doi.org/10.3109/02841859709171259>
  17. Wählin A, Holm J, Osterman G, Norberg B (1982) Evaluation of serial bone X-ray examination in multiple myeloma. *Acta Med Scand*. <https://doi.org/10.1111/j.0954-6820.1982.tb03234.x>
  18. Dinter DJ, Neff WK, Klaus J et al (2009) Comparison of whole-body MR imaging and conventional X-ray examination in patients with multiple myeloma and implications for therapy. *Ann Hematol*. <https://doi.org/10.1007/s00277-008-0621-6>
  19. Schreiman JS, McLeod RA, Kyle RA, Beabout JW (2014) Multiple myeloma: evaluation by CT. *Radiology*. <https://doi.org/10.1148/radiology.154.2.3966137>
  20. Mahnken AH, Wildberger JE, Gehbauer G et al (2002) Multidetector CT of the spine in multiple myeloma: comparison with MR imaging and radiography. *Am J Roentgenol*. <https://doi.org/10.2214/ajr.178.6.1781429>
  21. Horger M, Claussen CD, Bross-Bach U et al (2005) Whole-body low-dose multidetector row-CT in the diagnosis of multiple myeloma: an alternative to conventional radiography. *Eur J Radiol*. <https://doi.org/10.1016/j.ejrad.2004.04.015>
  22. Kröpil P, Fenk R, Fritz LB et al (2008) Comparison of whole-body 64-slice multidetector computed tomography and conventional radiography in staging of multiple myeloma. *Eur Radiol*. <https://doi.org/10.1007/s00330-007-0738-3>
  23. Gleeson TG, Byrne B, Kenny P et al (2010) Image quality in low-dose multidetector computed tomography: a pilot study to assess feasibility and dose optimization in whole-body bone imaging. *Can Assoc Radiol J*. <https://doi.org/10.1016/j.carj.2010.01.003>
  24. Rajkumar SV, Dimopoulos MA, Palumbo A et al (2014) International myeloma working group updated criteria for the diagnosis of multiple myeloma. *Lancet Oncol*
  25. Horger M, Pereira P, Claussen CD et al (2008) Hyperattenuating bone marrow abnormalities in myeloma patients using whole-body non-enhanced low-dose MDCT: Correlation with haematological parameters. *Br J Radiol*. <https://doi.org/10.1259/bjr/21850180>
  26. Hillengass J, Mouloupoulos LA, Delorme S, Koutoulidis V, Mosebich J, Hielscher T, Drake M, Rajkumar SV, Oestergaard B, Abildgaard N, Hinge M, Plesner T, Suehara Y, Matsue K, Withofs N, Caers J, Waage A, Goldschmidt H, Dimopoulos MA, Lentzsch S, Durie B, Terpos E (2017) Whole-body computed tomography versus conventional skeletal survey in patients with multiple myeloma: a study of the International Myeloma Working Group. *Blood Cancer J* 7. <https://doi.org/10.1038/bcj.2017.78>
  27. Husband JE, Schwartz LH, Spencer J et al (2004) Evaluation of the response to treatment of solid tumours - a consensus statement of the International Cancer Imaging Society. In: *British Journal of Cancer*
  28. Zambello R, Crimi F, Lico A, Barilà G, Branca A, Guolo A, Varin C, Vezzaro R, Checuz L, Scapin V, Berno T, Pizzi M, Ponzoni A, Biasi E, Vio S, Semenzato G, Zucchetto P, Lacognata C (2019) Whole-body low-dose CT recognizes two distinct patterns of lytic lesions in multiple myeloma patients with different disease metabolism at PET/MRI. *Ann Hematol* 98:679–689. <https://doi.org/10.1007/s00277-018-3555-7>
  29. Ippolito D, Besostri V, Bonaffini PA et al (2013) Diagnostic value of whole-body low-dose computed tomography(WBLDCT) in bone lesions detection in patients with multiplemyeloma (MM). *Eur J Radiol*. <https://doi.org/10.1016/j.ejrad.2013.08.036>
  30. Rajkumar SV (2015) Evolving diagnostic criteria for multiple myeloma. *Hematology*
  31. Heß T, Egerer G, Kasper B et al (2006) Atypical manifestations of multiple myeloma: radiological appearance. *Eur J Radiol*. <https://doi.org/10.1016/j.ejrad.2005.11.015>
  32. Gleeson TG, Moriarty J, Shortt CP et al (2009) Accuracy of whole-body low-dose multidetector CT (WBLDCT) versus skeletal survey in the detection of myelomatous lesions, and correlation of disease distribution with whole-body MRI (WBMRI). *Skelet Radiol*. <https://doi.org/10.1007/s00256-008-0607-4>
  33. Johnson TRC (2012) Dual-energy CT: general principles. *AJR Am J Roentgenol*
  34. Johnson TRC, Krauß B, Sedlmair M et al (2007) Material differentiation by dual energy CT: Initial experience. *Eur Radiol*. <https://doi.org/10.1007/s00330-006-0517-6>
  35. Rutherford RA, Pullan BR, Isherwood I (1976) X-ray energies for effective atomic number determination. *Neuroradiology*. 11:23–28. <https://doi.org/10.1007/BF00327254>
  36. Alvarez RE, MacOvski A (1976) Energy-selective reconstructions in X-ray computerised tomography. *Phys Med Biol*. <https://doi.org/10.1088/0031-9155/21/5/002>
  37. Kosmala A, Weng AM, Heidemeier A et al (2017) Multiple myeloma and dual-energy CT: diagnostic accuracy of virtual noncalcium technique for detection of bone marrow infiltration of the spine and pelvis. *Radiology*. <https://doi.org/10.1148/radiol.2017170281>
  38. Thomas C, Schabel C, Krauss B et al (2015) Dual-energy CT: virtual calcium subtraction for assessment of bone marrow involvement of the spine in multiple myeloma. In: *American Journal of Roentgenology*
  39. Kosmala A, Weng AM, Krauss B, Knop S, Bley TA, Petritsch B (2018) Dual-energy CT of the bone marrow in multiple myeloma: diagnostic accuracy for quantitative differentiation of infiltration patterns. *Eur Radiol* 28:5083–5090. <https://doi.org/10.1007/s00330-018-5537-5>
  40. Yu Z, Leng S, Jorgensen SM et al (2016) Evaluation of conventional imaging performance in a research whole-body CT system with a photon-counting detector array. *Phys Med Biol*. <https://doi.org/10.1088/0031-9155/61/4/1572>
  41. Goo HW, Goo JM (2017) Dual-energy CT: new horizon in medical imaging. *Korean J Radiol*
  42. Zamagni E, Nanni C, Patriarca F et al (2007) A prospective comparison of 18F-fluorodeoxyglucose positron emission tomography-computed tomography, magnetic resonance imaging and whole-body planar radiographs in the assessment of bone disease in newly diagnosed multiple myeloma. *Haematologica*. <https://doi.org/10.3324/haematol.10554>



43. Hillengass J, Landgren O (2013) Challenges and opportunities of novel imaging techniques in monoclonal plasma cell disorders: imaging early myeloma. *Leuk Lymphoma*
44. Walker R, Barlogie B, Haessler J et al (2007) Magnetic resonance imaging in multiple myeloma: diagnostic and clinical implications. *J Clin Oncol*. <https://doi.org/10.1200/JCO.2006.08.5803>
45. Regelink JC, Minnema MC, Terpos E et al (2013) Comparison of modern and conventional imaging techniques in establishing multiple myeloma-related bone disease: a systematic review. *Br J Haematol*. <https://doi.org/10.1111/bjh.12346>
46. Rasche L, Angtuaco E, McDonald JE et al (2017) Low expression of hexokinase-2 is associated with false-negative FDG-positron emission tomography in multiple myeloma. *Blood*. <https://doi.org/10.1182/blood-2017-03-774422>
47. Lindsey JD, Becker PS, Conrad EU (2016) My Myeloma : eloma : diagnosis and management. NICE Guidel
48. Hillengass J, Fechtner K, Weber MA et al (2010) Prognostic significance of focal lesions in whole-body magnetic resonance imaging in patients with asymptomatic multiple myeloma. *J Clin Oncol*. <https://doi.org/10.1200/JCO.2009.25.5356>
49. Rajkumar SV (2016) Myeloma today: disease definitions and treatment advances. *Am J Hematol*. <https://doi.org/10.1002/ajh.24236>
50. Rahmouni A, Divine M, Mathieu D et al (1993) Detection of multiple myeloma involving the spine: efficacy of fat-suppression and contrast-enhanced MR imaging. *Am J Roentgenol*. <https://doi.org/10.2214/ajr.160.5.8470574>
51. Ma J (2008) A single-point dixon technique for fat-suppressed fast 3D gradient-echo imaging with a flexible echo time. *J Magn Reson Imaging*. <https://doi.org/10.1002/jmri.21281>
52. Shah LM, Hanrahan CJ (2011) MRI of spinal bone marrow: part 1, techniques and normal age-related appearances. *Am J Roentgenol*
53. Dixon WT (1984) Simple proton spectroscopic imaging. *Radiology*. <https://doi.org/10.1148/radiology.153.1.6089263>
54. Yoo HJ, Hong SH, Kim DH et al (2017) Measurement of fat content in vertebral marrow using a modified dixon sequence to differentiate benign from malignant processes. *J Magn Reson Imaging*. <https://doi.org/10.1002/jmri.25496>
55. Kirchgessner T, Perlepe V, Michoux N et al (2017) Fat suppression at 2D MR imaging of the hands: Dixon method versus CHESSTechnique and STIR sequence. *Eur J Radiol*. <https://doi.org/10.1016/j.ejrad.2017.01.011>
56. Guerini H, Omoumi P, Guichoux F et al (2015) Fat suppression with Dixon techniques in musculoskeletal magnetic resonance imaging: a pictorial review. *Semin Musculoskelet Radiol*
57. van Vucht N, Santiago R, Lottmann B et al (2019) The Dixon technique for MRI of the bone marrow. *Skelet Radiol*
58. Bray TJP, Singh S, Latifoltojar A et al (2017) Diagnostic utility of whole body Dixon MRI in multiple myeloma: a multi-reader study. *PLoS One*. <https://doi.org/10.1371/journal.pone.0180562>
59. Lee S, Choi DS, Shin HS et al (2018) FSE T2-weighted two-point dixon technique for fat suppression in the lumbar spine: comparison with SPAIR technique. *Diagn Interv Radiol*. <https://doi.org/10.5152/dir.2018.17320>
60. Huijgen WHF, van Rijswijk CSP, Bloem JL (2019) Is fat suppression in T1 and T2 FSE with mDixon superior to the frequency selection-based SPAIR technique in musculoskeletal tumor imaging? *Skelet Radiol* 48:1905–1914. <https://doi.org/10.1007/s00256-019-03227-8>
61. Danner A, Brumpt E, Alilet M et al (2019) Improved contrast for myeloma focal lesions with T2-weighted Dixon images compared to T1-weighted images. *Diagn Interv Imaging*. <https://doi.org/10.1016/j.diii.2019.05.001>
62. Maeder Y, Dunet V, Richard R et al (2018) Bone marrow metastases: T2-weighted Dixon spin-echo fat images can replace T1-weighted spin-echo images. *Radiology*. <https://doi.org/10.1148/radiol.2017170325>
63. Messiou C, Hillengass J, Delorme S et al (2019) Guidelines for acquisition, interpretation, and reporting of whole-body MRI in myeloma: myeloma response assessment and diagnosis system (MY-RADS). *Radiology*. <https://doi.org/10.1148/radiol.2019181949>
64. Silva JR, Hayashi D, Yonenaga T et al (2013) MRI of bone marrow abnormalities in hematological malignancies. *Diagn Interv Radiol*. <https://doi.org/10.5152/dir.2013.067>
65. Dutoit JC, Vanderkerken MA, Anthonissen J, Dochy F, Verstraete KL (2014) The diagnostic value of SE MRI and DWI of the spine in patients with monoclonal gammopathy of undetermined significance, smoldering myeloma and multiple myeloma. *Eur Radiol* 24:2754–2765. <https://doi.org/10.1007/s00330-014-3324-5>
66. Alyas F, Saifuddin A, Connell D (2007) MR imaging evaluation of the bone marrow and marrow infiltrative disorders of the lumbar spine. *Magn Reson Imaging Clin N Am*
67. Baur-Melnyk A, Buhmann S, Dürr HR, Reiser M (2005) Role of MRI for the diagnosis and prognosis of multiple myeloma. *Eur J Radiol*. <https://doi.org/10.1016/j.ejrad.2005.01.017>
68. Stähler A, Baur A, Bartl R et al (1996) Contrast enhancement and quantitative signal analysis in MR imaging of multiple myeloma: assessment of focal and diffuse growth patterns in marrow correlated with biopsies and survival rates. *Am J Roentgenol*. <https://doi.org/10.2214/ajr.167.4.8819407>
69. Lecouvet FE, Vande Berg BC, Michaux L et al (2014) Stage III multiple myeloma: clinical and prognostic value of spinal bone marrow MR imaging. *Radiology*. <https://doi.org/10.1148/radiology.209.3.9844655>
70. Caers J, Withofs N, Hillengass J et al (2014) The role of positron emission tomography-computed tomography and magnetic resonance imaging in diagnosis and follow up of multiple myeloma. *Haematologica*
71. Baliyan V, Das CJ, Sharma R, Gupta AK (2016) Diffusion weighted imaging: technique and applications. *World J Radiol*. <https://doi.org/10.4329/wjr.v8.i9.785>
72. Kwee TC, Takahara T, Ochiai R et al (2008) Diffusion-weighted whole-body imaging with background body signal suppression (DWIBS): features and potential applications in oncology. *Eur Radiol*. <https://doi.org/10.1007/s00330-008-0968-z>
73. Messiou C, Giles S, Collins DJ et al (2012) Assessing response of myeloma bone disease with diffusion-weighted MRI. *Br J Radiol*. <https://doi.org/10.1259/bjr/52759767>
74. Messiou C, Kaiser M (2015) Whole body diffusion weighted MRI - a new view of myeloma. *Br J Haematol*
75. Huang S-Y, Chen B-B, Lu H-Y et al (2012) Correlation among DCE-MRI measurements of bone marrow angiogenesis, microvessel density, and extramedullary disease in patients with multiple myeloma. *Am J Hematol*. <https://doi.org/10.1002/ajh.23256>
76. Messiou C, Collins DJ, Morgan VA, Desouza NM (2011) Optimising diffusion weighted MRI for imaging metastatic and myeloma bone disease and assessing reproducibility. *Eur Radiol*. <https://doi.org/10.1007/s00330-011-2116-4>
77. Padhani AR, Van Ree K, Collins DJ et al (2013) Assessing the relation between bone marrow signal intensity and apparent diffusion coefficient in diffusion-weighted MRI. *Am J Roentgenol*. <https://doi.org/10.2214/AJR.11.8185>
78. Perez-Lopez R, Rodrigues DN, Figueiredo I et al (2018) Multiparametric magnetic resonance imaging of prostate cancer bone disease correlation with bone biopsy histological and molecular features. *Investig Radiol*. <https://doi.org/10.1097/RLI.0000000000000415>
79. Winfield JM, Poillucci G, Blackledge MD, Collins DJ, Shah V, Tunariu N, Kaiser MF, Messiou C (2018) Apparent diffusion





- coefficient of vertebral haemangiomas allows differentiation from malignant focal deposits in whole-body diffusion-weighted MRI. *Eur Radiol* 28:1687–1691. <https://doi.org/10.1007/s00330-017-5079-2>
80. Dutoit JC, Verstraete KL (2016) MRI in multiple myeloma: a pictorial review of diagnostic and post-treatment findings. *Insights Imaging*
  81. Lacognata C, Crimi F, Guolo A et al (2017) Diffusion-weighted whole-body MRI for evaluation of early response in multiple myeloma. *Clin Radiol*. <https://doi.org/10.1016/j.crad.2017.05.004>
  82. Pearce T, Philip S, Brown J et al (2012) Bone metastases from prostate, breast and multiple myeloma: differences in lesion conspicuity at short-tau inversion recovery and diffusion-weighted MRI. *Br J Radiol*. <https://doi.org/10.1259/bjr/30649204>
  83. Terpos E, Kleber M, Engelhardt M et al (2015) European myeloma network guidelines for the management of multiple myeloma-related complications. *Haematologica*. <https://doi.org/10.3324/haematol.2014.117176>
  84. Wu LM, Gu HY, Zheng J et al (2011) Diagnostic value of whole-body magnetic resonance imaging for bone metastases: a systematic review and meta-analysis. *J Magn Reson Imaging*. <https://doi.org/10.1002/jmri.22608>
  85. Lecouvet FE, El Mouedden J, Collette L et al (2012) Can whole-body magnetic resonance imaging with diffusion-weighted imaging replace tc 99m bone scanning and computed tomography for single-step detection of metastases in patients with high-risk prostate cancer? *Eur Urol*. <https://doi.org/10.1016/j.eururo.2012.02.020>
  86. Hillengass J, Stoll J, Zechmann CM, Kunz C, Wagner B, Heiss C, Sumkaskaite M, Moehler TM, Schlemmer HP, Goldschmidt H, Delorme S (2015) The application of Gadopentate-Dimreneglumine has no impact on progression free and overall survival as well as renal function in patients with monoclonal plasma cell disorders if general precautions are taken. *Eur Radiol* 25:745–750. <https://doi.org/10.1007/s00330-014-3458-5>
  87. Verstraete KL, Van der Woude H-J, Hogendoorn PCW et al (2007) Dynamic contrast-enhanced MR imaging of musculoskeletal tumors: basic principles and clinical applications. *J Magn Reson Imaging*. <https://doi.org/10.1002/jmri.1880060210>
  88. Dutoit JC, Vanderkerken MA, Verstraete KL (2013) Value of whole body MRI and dynamic contrast enhanced MRI in the diagnosis, follow-up and evaluation of disease activity and extent in multiple myeloma. *Eur J Radiol*. <https://doi.org/10.1016/j.ejrad.2013.04.012>
  89. Lavini C, de Jonge MC, van de Sande MGH et al (2007) Pixel-by-pixel analysis of DCE MRI curve patterns and an illustration of its application to the imaging of the musculoskeletal system. *Magn Reson Imaging*. <https://doi.org/10.1016/j.mri.2006.10.021>
  90. Garcia-Figueiras R, Padhani AR, Beer AJ et al (2015) Imaging of tumor angiogenesis for radiologists-part 1: biological and technical basis. *Curr Probl Diagn Radiol*
  91. Dimopoulos MA, Hillengass J, Usmani S et al (2015) Role of magnetic resonance imaging in the management of patients with multiple myeloma: a consensus statement. *J Clin Oncol*. <https://doi.org/10.1200/JCO.2014.57.9961>
  92. Boellaard R, Delgado-Bolton R, Oyen WJG, et al (2015) FDG PET/CT: EANM procedure guidelines for tumour imaging: version 2.0. *Eur J Nucl Med Mol Imaging*
  93. Valls L, Badve C, Avril S et al (2016) FDG-PET imaging in hematological malignancies. *Blood Rev*
  94. Weiler-Sagie M, Bushelev O, Epelbaum R et al (2010) 18F-FDG avidity in lymphoma readdressed: a study of 766 patients. *J Nucl Med*. <https://doi.org/10.2967/jnumed.109.067892>
  95. El Arfani C, De Veirman K, Maes K et al (2018) Metabolic features of multiple myeloma. *Int J Mol Sci*
  96. Zhang XD, Deslandes E, Villedieu M et al (2006) Effect of 2-deoxy-D-glucose on various malignant cell lines in vitro. *Anticancer Res*
  97. Zhang D, Li J, Wang F et al (2014) 2-Deoxy-D-glucose targeting of glucose metabolism in cancer cells as a potential therapy. *Cancer Lett*
  98. Bolzoni M, Chiu M, Accardi F et al (2016) Dependence on glutamine uptake and glutamine addiction characterize myeloma cells: a new attractive target. *Blood*. <https://doi.org/10.1182/blood-2016-01-690743>
  99. Moreau P, Attal M, Caillot D et al (2017) Prospective evaluation of magnetic resonance imaging and [18F]fluorodeoxyglucose positron emission tomography-computed tomography at diagnosis and before maintenance therapy in symptomatic patients with multiple myeloma included in the IFM/DFCI 2009 trial. In: *Journal of Clinical Oncology*
  100. Terpos E, Dimopoulos MA, Sezer O (2007) The effect of novel anti-myeloma agents on bone metabolism of patients with multiple myeloma. *Leukemia*
  101. Zamagni E, Patriarca F, Nanni C et al (2011) Prognostic relevance of 18-F FDG PET/CT in newly diagnosed multiple myeloma patients treated with up-front autologous transplantation. *Blood*. <https://doi.org/10.1182/blood-2011-06-361386>
  102. Bannas P, Hentschel HB, Bley TA et al (2012) Diagnostic performance of whole-body MRI for the detection of persistent or relapsing disease in multiple myeloma after stem cell transplantation. *Eur Radiol*. <https://doi.org/10.1007/s00330-012-2445-y>
  103. Cavo M, Terpos E, Nanni C et al (2017) Role of 18F-FDG PET/CT in the diagnosis and management of multiple myeloma and other plasma cell disorders: a consensus statement by the International Myeloma Working Group. *Lancet Oncol*
  104. Lückereath K, Lapa C, Albert C et al (2015) 11C-methionine-PET: a novel and sensitive tool for monitoring of early response to treatment in multiple myeloma. *Oncotarget*. <https://doi.org/10.18632/oncotarget.3053>
  105. Ho CL, Chen S, Leung YL et al (2014) 11C-acetate PET/CT for metabolic characterization of multiple myeloma: a comparative study with 18F-FDG PET/CT. *J Nucl Med*. <https://doi.org/10.2967/jnumed.113.131169>
  106. Brigle K, Pierre A, Finley-Oliver E et al (2017) Myelosuppression, bone disease, and acute renal failure: evidence-based recommendations for oncologic emergencies. *Clin J Oncol Nurs*
  107. Terpos E, Christoulas D, Gavriatopoulou M (2018) Biology and treatment of myeloma related bone disease. *Metabolism*. <https://doi.org/10.1016/j.metabol.2017.11.012>
  108. Avva R, Vanhemert RL, Barlogie B et al (2001) CT-guided biopsy of focal lesions in patients with multiple myeloma may reveal new and more aggressive cytogenetic abnormalities. *Am J Neuroradiol*
  109. Mink J (1986) Percutaneous bone biopsy in the patient with known or suspected osseous metastases. *Radiology*. <https://doi.org/10.1148/radiology.161.1.3763865>
  110. Thumallapally N, Meshref A, Mousa M, Terjanian T (2017) Solitary plasmacytoma: population-based analysis of survival trends and effect of various treatment modalities in the USA. *BMC Cancer*. <https://doi.org/10.1186/s12885-016-3015-5>
  111. Dimopoulos M, Kyle R, Fermand JP et al (2011) Consensus recommendations for standard investigative workup: report of the International Myeloma Workshop Consensus Panel 3. In: *Blood*
  112. Engelhardt M, Udi J, Kleber M et al (2010) European myeloma network: the 3rd Trialist forum consensus statement from the European experts meeting on multiple myeloma. *Leuk Lymphoma*
  113. Melton LJ, Crowson CS, O'Fallon WM (1999) Fracture incidence in Olmsted County, Minnesota: Comparison of urban with rural rates and changes in urban rates over time. *Osteoporos Int*. <https://doi.org/10.1007/s001980050113>

114. Melton LJ, Kyle RA, Achenbach SJ et al (2005) Fracture risk with multiple myeloma: a population-based study. *J Bone Miner Res*. <https://doi.org/10.1359/JBMR.041131>
115. Cotten A, Dewatre F, Cortet B et al (1996) Percutaneous vertebroplasty for osteolytic metastases and myeloma: effects of the percentage of lesion filling and the leakage of methyl methacrylate at clinical follow-up. *Radiology*. <https://doi.org/10.1148/radiology.200.2.8685351>
116. Ha KY, Kim YH, Kim HW (2013) Multiple myeloma and epidural spinal cord compression: case presentation and a spine surgeon's perspective. *J Korean Neurosurg Soc*. <https://doi.org/10.3340/jkns.2013.54.2.151>
117. Wallington M, Mendis S, Premawardhana U et al (1997) Local control and survival in spinal cord compression from lymphoma and myeloma. *Radiother Oncol*. [https://doi.org/10.1016/S0167-8140\(96\)01858-0](https://doi.org/10.1016/S0167-8140(96)01858-0)
118. Kyriakou C, Molloy S, Vrionis F, Alberico R, Bastian L, Zonder JA, Giralt S, Raje N, Kyle RA, Roodman DGD, Dimopoulos MA, Rajkumar SV, Durie BBG, Terpos E (2019) The role of cement augmentation with percutaneous vertebroplasty and balloon kyphoplasty for the treatment of vertebral compression fractures in multiple myeloma: a consensus statement from the International Myeloma Working Group (IMWG). *Blood Cancer J* 9:1–10. <https://doi.org/10.1038/s41408-019-0187-7>
119. Soutar R, Lucraft H, Jackson G et al (2004) Guidelines on the diagnosis and management of solitary plasmacytoma of bone and solitary extramedullary plasmacytoma. *Br J Haematol*
120. Baerlocher MO, Saad WE, Dariushnia S et al (2014) Quality improvement guidelines for percutaneous vertebroplasty. *J Vasc Interv Radiol*. <https://doi.org/10.1016/j.jvir.2013.09.004>
121. Jensen ME, McGraw JK, Cardella JF (2011) Position statement on percutaneous vertebral augmentation: a consensus statement developed by the American Society of Interventional and Therapeutic Neuroradiology, Society of Interventional Radiology, American Association of Neurological Surgeons/Congres. *J Neurointerv Surg*
122. Calmels V, Vallée JN, Rose M, Chiras J (2007) Osteoblastic and mixed spinal metastases: evaluation of the analgesic efficacy of percutaneous vertebroplasty. *Am J Neuroradiol*. [https://doi.org/10.1016/s1073-5437\(08\)70967-7](https://doi.org/10.1016/s1073-5437(08)70967-7)
123. Zheng L, Chen Z, Sun M et al (2014) A preliminary study of the safety and efficacy of radiofrequency ablation with percutaneous kyphoplasty for thoracolumbar vertebral metastatic tumor treatment. *Med Sci Monit*. <https://doi.org/10.12659/MSM.889742>
124. Wallace AN, Greenwood TJ, Jennings JW (2015) Radiofrequency ablation and vertebral augmentation for palliation of painful spinal metastases. *J Neuro-Oncol*. <https://doi.org/10.1007/s11060-015-1813-2>
125. Erdem E, Akdol S, Amole A et al (2013) Radiofrequency-targeted vertebral augmentation for the treatment of vertebral compression fractures as a result of multiple myeloma. *Spine (Phila Pa 1976)*. <https://doi.org/10.1097/BRS.0b013e3182959695>
126. Barbero S, Casorzo I, Durando M, Mattone G, Tappero C, Venturi C, Gandini G (2008) Percutaneous vertebroplasty: the follow-up. *Radiol Med* 113:101–113. <https://doi.org/10.1007/s11547-008-0234-0>
127. Gozzetti A, Cerase A, Defina M, Bocchia M (2012) Plasmacytoma of the skull. *Eur J Haematol*
128. Cerase A, Tarantino A, Gozzetti A et al (2008) Intracranial involvement in plasmacytomas and multiple myeloma: a pictorial essay. *Neuroradiology*
129. Gozzetti A, Cerase A, Tarantino A et al (2007) Multiple myeloma involving the cavernous sinus: a report of 3 cases and response to bortezomib. *Clin Lymphoma Myeloma*. <https://doi.org/10.3816/CLM.2007.n.017>
130. Jurczynszyn A, Grzasko N, Gozzetti A et al (2016) Central nervous system involvement by multiple myeloma: a multi-institutional retrospective study of 172 patients in daily clinical practice. *Am J Hematol*. <https://doi.org/10.1002/ajh.24351>
131. Rosenberg S, Shapur N, Gofrit O, Or R (2010) Plasmacytoma of the testis in a patient with previous multiple myeloma: is the testis a sanctuary site? *J Clin Oncol*. <https://doi.org/10.1200/JCO.2009.27.6519>
132. Anghel G, Petti N, Remotti D et al (2002) Testicular plasmacytoma: report of a case and review of the literature. *Am J Hematol*. <https://doi.org/10.1002/ajh.10174>
133. Gozzetti A, Cerase A, Lotti F et al (2012) Extramedullary intracranial localization of multiple myeloma and treatment with novel agents: a retrospective survey of 50 patients. *Cancer*. <https://doi.org/10.1002/cncr.26447>
134. Ooi GC, Chim JCS, Au WY, Khong PL (2006) Radiologic manifestations of primary solitary extramedullary and multiple solitary plasmacytomas. *Am J Roentgenol*
135. Sancharawala V (2006) Light-chain (AL) amyloidosis: diagnosis and treatment. *Clin J Am Soc Nephrol*
136. Lee SP, Park JB, Kim HK et al (2019) Contemporary imaging diagnosis of cardiac amyloidosis. *J Cardiovasc Imaging*
137. Palladini G, Hegenbart U, Milani P et al (2014) A staging system for renal outcome and early markers of renal response to chemotherapy in AL amyloidosis. *Blood*. <https://doi.org/10.1182/blood-2014-04-570010>
138. Kawashima A, Alleman WG, Takahashi N et al (2011) Imaging evaluation of amyloidosis of the urinary tract and retroperitoneum. *Radiographics*. <https://doi.org/10.1148/rg.316115519>
139. Czeyda-Pommersheim F, Hwang M, Chen SS et al (2015) Amyloidosis: modern cross-sectional imaging. *Radiographics*. <https://doi.org/10.1148/rg.2015140179>
140. Dispenzieri A (2017) POEMS syndrome: 2017 update on diagnosis, risk stratification, and management. *Am J Hematol*. <https://doi.org/10.1002/ajh.24802>
141. Paiva B, Garcia-Sanz R, San Miguel JF (2016) Multiple myeloma minimal residual disease. In: *Cancer Treatment and Research*
142. Kumar S, Paiva B, Anderson KC et al (2016) International Myeloma Working Group consensus criteria for response and minimal residual disease assessment in multiple myeloma. *Lancet Oncol*

143. Zamagni E, Cavo M (2012) The role of imaging techniques in the management of multiple myeloma. *Br J Haematol*

**Publisher's note** Springer Nature remains neutral with regard to jurisdictional claims in published maps and institutional affiliations.

## Affiliations

Francesca Di Giuliano<sup>1</sup>  · Eliseo Picchi<sup>2,3</sup>  · Massimo Muto<sup>4,5</sup>  · Antonello Calcagni<sup>2,3</sup>  · Valentina Ferrazzoli<sup>1</sup>  · Valerio Da Ros<sup>3,6</sup>  · Silvia Minosse<sup>3</sup>  · Agostino Chiaravalloti<sup>3,7</sup>  · Francesco Garaci<sup>1,8</sup>  · Roberto Floris<sup>2,3</sup>  · Mario Muto<sup>5</sup> 

<sup>1</sup> Neuroradiology Unit, Department of Biomedicine and Prevention, University of Rome Tor Vergata, 00133 Rome, Italy

<sup>2</sup> Diagnostic Imaging Unit, Integrated Care Processes Department, Policlinico Tor Vergata, 00133 Rome, Italy

<sup>3</sup> Department of Biomedicine and Prevention, University of Rome Tor Vergata, 00133 Rome, Italy

<sup>4</sup> Department of Neurosciences and Reproductive and Odontostomatological Sciences, University of Naples Federico II, 80100 Naples, Italy

<sup>5</sup> Department of Neuroradiology, A.O.R.N. Cardarelli, 80100 Naples, Italy

<sup>6</sup> Integrated Care Processes Department, Interventional Radiology Unit, Policlinico Tor Vergata, 00133 Rome, Italy

<sup>7</sup> IRCCS Neuromed, Pozzilli, Italy

<sup>8</sup> San Raffaele Cassino, Cassino, FR, Italy